

# Characterization of TiAl based alloys with various content of carbon

A Klimová, J Lapin and T Pelachová

Institute of Materials and Machine Mechanics, Slovak Academy of Sciences,  
Dúbravská cesta 9, 845 13 Bratislava 3, Slovak Republic

E-mail: ummsakli@savba.sk

**Abstract.** TiAl based alloys prepared by induction melting with nominal compositions Ti-(37.5-41)Al-(3.5-4)Nb-1Mo-0.1B-xC (at.%), where carbon content x is ranging from 3 to 7 at.%, were characterised by optical microscopy (OM), scanning electron microscopy (SEM), energy dispersive spectroscopy (EDS), X-ray diffraction analysis (XRD) and elemental LECO analysers of light elements (O, N and C). Morphology and volume fraction of coexisting phases are quantitatively analysed using computerised image analyser. The effect of carbon content on Vickers microhardness and hardness of the alloys is evaluated and discussed. The microstructure of the alloys consists of fine-grained lamellar matrix with elongated Ti<sub>2</sub>AlC particles dispersed in the whole volume of the ingots. The volume fraction of the carbide particles increases with the carbon content of the studied alloys from 8 to 18 vol.%. The average Vickers hardness of the ingots doesn't show the significant variations with their carbon content, but the hardness considerably exceeds the average values in the surface regions where the small rod shape particles are densely distributed in the matrix.

## 1 Introduction

In the last decades the big attention was paid to the developing of new  $\gamma$ -TiAl based intermetallic alloys due to their very promising properties for high temperature applications in automotive, aircraft and power industry [1]. Several processing techniques and various alloying elements have been investigated to improve their room temperature low ductility and fracture toughness, oxidation resistance at high temperatures, creep properties and raise their current operational temperature limit over 750°C [2]. Beside the additions of elements such as Mo, Nb, Ta, W, Zr or Cr, which affect the properties of these alloys through the solution hardening and changes of the microstructure, the addition of the appropriate amounts of carbon can lead to the formation of reinforcing carbide particles which can have the positive effect on mechanical properties of the final alloy at both ambient and elevated temperatures [3, 4].

The aim of the present work is to characterize chemical composition, microstructure and Vickers hardness of the TiAl based alloys with nominal compositions Ti-(37.5-41)Al-(3.5-4)Nb-1Mo-0.1B-xC (at.%) prepared by the induction melting in graphite crucibles. The carbon content x is varied from 3 to 7 at.%. Because of low solubility of carbon [5] in main coexisting phases present in the TiAl based alloy such as  $\alpha_2$ (Ti<sub>3</sub>Al),  $\gamma$ (TiAl) and  $\beta$ (Ti), the selected alloying with C is expected to affect solidification path and favour formation of primary carbide particles in the studied alloys during solidification [5, 6].



## 2 Experimental procedure

The experimental TiAl based alloys with nominal compositions Ti-(37.5-41)Al-(3.5-4)Nb-1Mo-0.1B-(3-7)C (at.%) were prepared by induction melting in graphite crucibles followed by solidification under argon atmosphere. Cylindrical ingots with a diameter of 42 mm and length of 15 mm were cut longitudinally using wire electrical discharge machining. Microstructural investigations were performed by optical microscopy (OM), scanning electron microscopy (SEM) and X-ray diffraction analysis (XRD). Chemical composition of the alloys was analyzed by energy-dispersive spectrometry (EDS) using JSM-6510 scanning electron microscope equipped with EDS detector. For measurements of oxygen and nitrogen content, LECO ONH836 Elemental Analyzer was used. The analysis of carbon content was performed by LECO CS844 Elemental Analyzer. OM, SEM, XRD and EDS samples were prepared using standard grinding and polishing metallographic techniques. After mechanical polishing the samples for OM were chemically etched in a reagent consisting of 100 ml H<sub>2</sub>O, 10 ml HNO<sub>3</sub> and 3 ml HF. Vickers hardness and Vickers microhardness measurements were performed on polished and slightly etched surfaces at an applied load of 294 N (HV30) and 0.098 N (HV<sub>m</sub>), respectively. Grain size, volume fraction of the coexisting phases and interlamellar  $\alpha_2$ - $\alpha_2$  spacing were determined from the digitalized micrographs using computer image analyzer.

## 3 Results and discussion

The average chemical composition of the investigated alloys measured by EDS is shown in the table 1. Because of the limitation of EDS method in measuring of light elements, the content of boron is taken from independent analysis to be 0.1 at.% of the master alloy. The average content of O, N and C measured by the elemental analysers LECO in the central part of the ingots is shown in the table 2. Because of the expected inhomogeneity in the carbon content due to the effect of the graphite crucible, the carbon content was analysed also in the vicinity of the surface connected with the crucible during melting. As seen in table 1, only slight increase of carbon content in the surface regions in comparison with the central part is detected in the ingots TiAl-3C and TiAl-5C alloyed with 3 and 5 at.% of C. On the contrary, the ingot TiAl-7C shows the difference in carbon content between the central part and surface regions 3.3 at.%. This inhomogeneous distribution of carbon in the relationship with the inhomogeneity of microstructure of the ingots is discussed later in the paper.

**Table 1.** Chemical composition measured by EDS (at.%).

Ingot	Nominal composition	Al	Ti	Nb	Mo
TiAl-3C	Ti-41Al-4Nb-1Mo-0.1B-3C	40.82±0.10	52.69±0.14	4.36±0.05	1.08±0.12
TiAl-5C	Ti-39.5Al-3.5Nb-1Mo-0.1B-5C	39.25±0.29	53.67±0.30	4.28±0.07	1.13±0.10
TiAl-7C	Ti-37.5Al-3.5Nb-1Mo-0.1B-7C	37.92±1.02	54.16±1.18	4.07±0.18	0.96±0.12

**Table 2.** Content of O, N and C measured by the analysers of the light elements LECO.

Ingot	O (wt.%)	N (wt.%)	C (wt.% / at.%) centre	C (wt.% / at.%) surface region
TiAl-3C	0.0861	0.0284	0.87 / 2.60	0.93 / 2.80
TiAl-5C	0.0886	0.0490	1.50 / 4.50	1.60 / 4.80
TiAl-7C	0.0982	0.0719	1.90 / 5.70	3.00 / 9.00

### 3.1 Microstructure of the ingots

The microstructure of the studied alloys is composed of fine-grained lamellar  $\alpha_2$ (Ti<sub>3</sub>Al)+ $\gamma$ (TiAl) matrix,  $\beta$ -phase (Ti-based solid solution with cubic crystal structure), thin layer of  $\gamma$ -phase formed on the grain boundaries, boride particles and carbide particles dispersed in the whole volume of the ingots, as shown in figure 1a. XRD patterns in figure 1b indicate that the crystal structure of the carbides belongs to Ti<sub>2</sub>AlC phase. The Ti<sub>2</sub>AlC peaks in the XRD patterns increase with the increase of

carbon content, what is in a very good agreement with the results of Song et al. [7]. Formation of TiB and TiB<sub>2</sub> particles is also proved very well by the corresponding peaks in the XRD patterns in figure 1b.

The shape of the carbide particles is elongated. Their average aspect ratio (length/width) is measured to be 5.0 and 4.4 in the central part of the TiAl-3C and TiAl-7C ingots, respectively. In the vicinity of the surface connected with the crucible, the thin needle shaped particles with a length over 100  $\mu\text{m}$  are formed, especially in the ingot TiAl-3C (figure 2a). Large clusters of small rod shaped carbide particles with smooth surface and aspect ratio of about 2.5 are observed close to the surface of the TiAl-5C and TiAl-7C ingots (figure 2b).

The volume fraction of carbide particles increases from 8 vol.% in the TiAl-3C to 18 vol.% in the ingot TiAl-7C. The volume fraction of the  $\beta$ -phase varies between 7 and 10 vol.% in all three alloys.

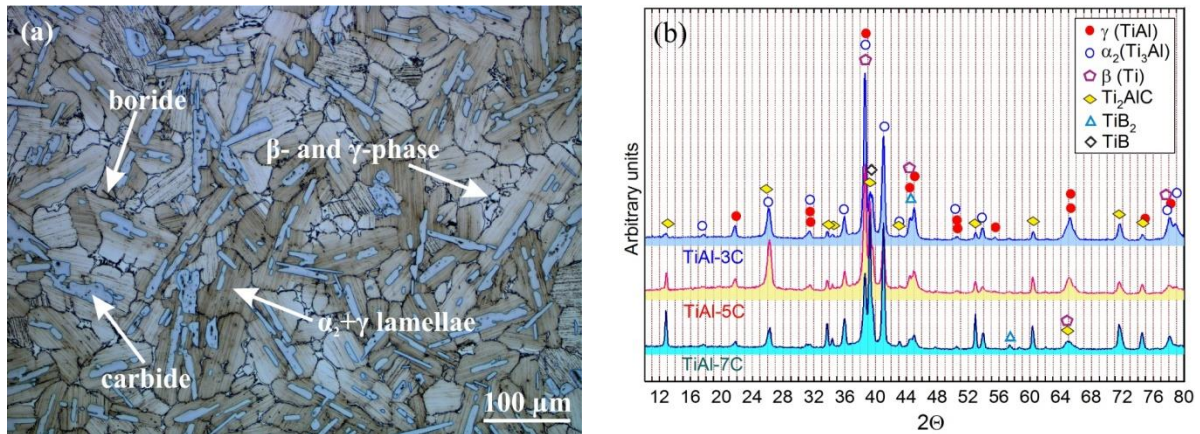


**Figure 1.** (a) Microstructure of the ingot TiAl-7C (OM); (b) XRD patterns of the ingots.

The lamellar grains in the central part of the ingots maintain the elongated shape of the carbide particles with the average length of around 80  $\mu\text{m}$  and aspect ratio of 2. Only in the surface regions with the extensive clusters of small rod shaped carbide particles, the morphology of grains is more equiaxed with the average size of (40  $\pm$  10)  $\mu\text{m}$ . The orientation of  $\alpha_2 + \gamma$  lamellae is parallel to the longitudinal axis of the carbide particles in the majority of grains, what indicates a defined crystallographic orientation relationship between the carbide particles and matrix formed during the solidification. The average interlamellar  $\alpha_2 - \alpha_2$  spacing is measured to be (300  $\pm$  20) nm in all studied ingots.

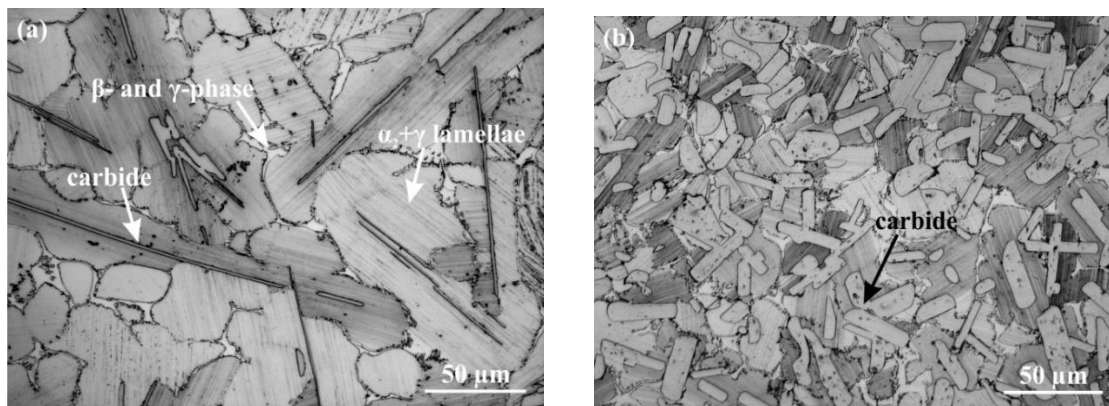


**Figure 2.** Microstructure of the ingots in the vicinity of the surface (OM) (a) TiAl-3C; (b) TiAl-7C.

### 3.2 Distribution of alloying elements

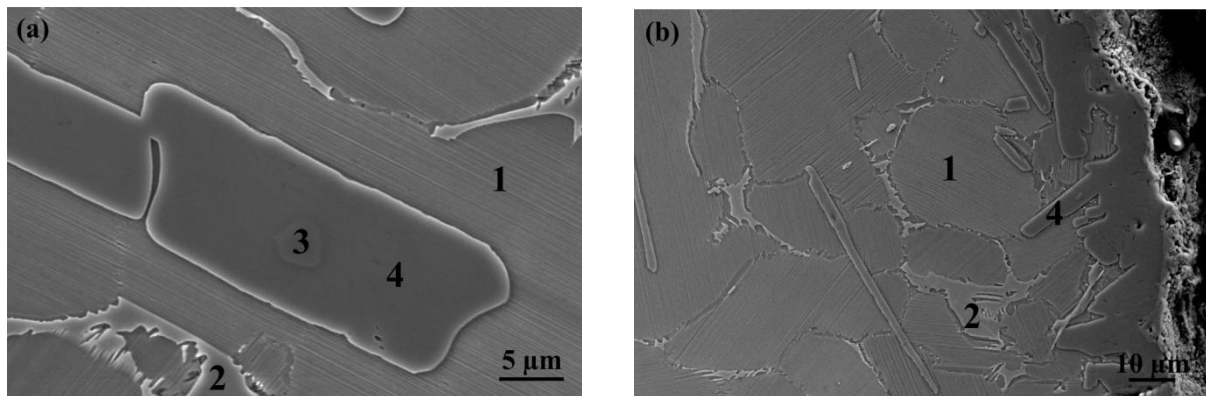
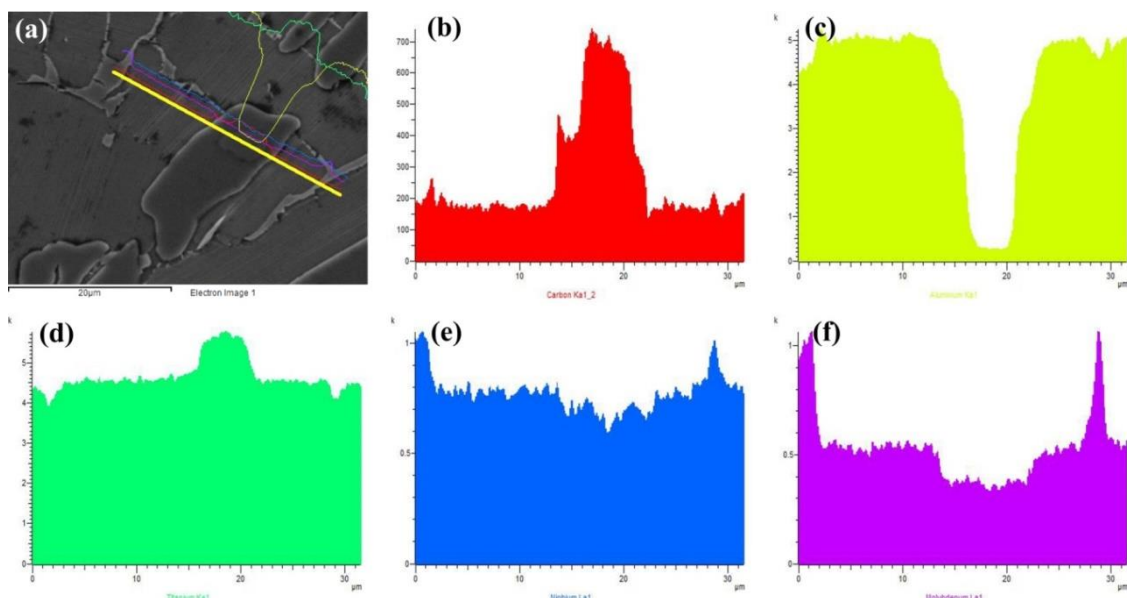
The chemical compositions of  $\alpha_2+\gamma$  lamellar grains,  $\beta$ -phase formed at the grain boundaries and carbide particles (figure 3) are shown in tables 3 and 4.

**Table 3.** Chemical composition of the matrix measured by EDS (at.%).

Position (figure 3)	Al	Ti	Nb	Mo
1	41.21±0.40	52.49±0.47	4.21±0.15	0.98±0.08
2	35.69±0.13	55.08±0.43	5.55±0.24	3.68±0.12

**Table 4.** Chemical composition of the carbide particles measured by EDS (at.%).

Position (figure 3)	C	Al	Ti	Nb	Mo
3	38.41±1.00	0.86±0.50	58.49±2.14	2.23±0.71	0.03±0.04
4	24.72±0.93	24.49±1.44	47.51±1.05	3.25±0.20	0.04±0.04

**Figure 3.**  $\alpha_2+\gamma$  lamellar grains (1),  $\beta$ -phase (2) and carbide particles (3, 4) (SEM); (a) in the center of the ingots; (b) in the vicinity of the surface connected with the crucible during the melting.

**Figure 4.** EDS line scan elemental profiles along the yellow line: (a) SEM image; (b) carbon, (c) aluminium, (d) titanium, (e) niobium, (f) molybdenum.

According to the atom probe tomography measurements of the local chemical composition of Ti-Al-Nb alloys with 0.5 - 0.75 at.% of C, reported in [8, 9], solubility limits of C in the  $\alpha_2$ ,  $\gamma$  and  $\beta$  phases reach the following 1.2 at.%, 0.25 - 0.3 at.% and 0.0 at.%, respectively. Because of the limitation of the EDS method applied in our study, low carbon content in the matrix of the studied alloys couldn't be measured precisely. However, as seen in figure 4b, the line scan across the all coexisting phases shows the presence of carbon not only in the carbide particles, but also its segregation on the  $\gamma/\beta$  interfaces and grain boundaries. The evidence of the accumulation of C in the vicinity of  $\gamma/\beta$  interface was reported also by Klein et al. [8].

For the measurements of the higher amounts of carbon in carbide particles, the standardization of the EDS analyzer on certified  $Ti_2AlC$  standard was used. The carbide particles are identified by EDS measurements and XRD analysis to belong to  $Ti_2AlC$  phase, as seen in table 4 and figure 1b. However, figure 3a and 4a indicates that the large carbide particles contain small central area enriched by carbon and depleted by Al. The similar core depleted by Al inside the particles was also observed in TiAl matrix composites prepared by arc-melting methods [7, 10, 11]. The surface layer shown in Figure 3b is formed by  $Ti_2AlC$  type of carbide, what was proved by both XRD patterns (figure 1b) and EDS measurements (table 4).

Nb and Mo as strong  $\beta$ -phase stabilizers [2] are concentrated on the grain boundaries, where the  $\beta$  phase is formed (figure 4e and 4f). Small increase of Nb in the  $\beta$  phase in comparison with the lamellar grains and three times higher content of Mo in the  $\beta$  phase than in the lamellar matrix (table 3) indicate the stronger stabilization effect of Mo than of Nb [7]. Carbide particles are free of Mo, but contain of about 3 at.% of Nb.

### 3.3 Hardness and microhardness

The average hardness HV30 of the ingots is not affected by the carbon content. All average values fall within the standard deviation interval of the measurements (table 5). Higher standard deviation of HV30 values in the TiAl-7 ingot is caused by the inhomogeneous distribution of the carbide particles and different size and morphology of the grains in the central part (figure 1a) and in the vicinity of the surface (figure 2b). While in the central part of the ingot TiAl-7C the average hardness is about 370 HV30, the hardness reaches the values over 400 HV30 in the regions with high density of small rod shape particles in the matrix with nearly equiaxed grains (figure 2b).

**Table 5.** Vickers hardness HV30 of the ingots and Vickers microhardness  $HV_m$  of the lamellar grains.

	TiAl-3C	TiAl-5C	TiAl-7C
HV30 of the ingots	386±9	384±6	385±16
$HV_m$ of the lamellar grains	562±37	576±42	588±22

The Vickers microhardness  $HV_m$  of the lamellar matrix is slightly increasing with the increase of the carbon content, but this increase is within the standard deviations of the measurements (table 5). The average microhardness of the  $\beta$ -phase in all three ingots reaches the same value of about 580±48  $HV_m$  as the lamellar matrix, and the microhardness of the carbide particles is determined to be around 800  $HV_m$ .

## 5 Conclusions

The achieved results of the study of TiAl based alloys with nominal compositions Ti-(37.5-41)Al-(3.5-4)Nb-1Mo-0.1B-(3-7)C (at.%) can be summarized as follows:

1. The microstructure of the studied alloys is composed of fine-grained  $\alpha_2(\text{Ti}_3\text{Al})+\gamma(\text{TiAl})$  lamellar matrix with the  $\beta$ -phase and thin layer of  $\gamma$ -phase formed on the grain boundaries and  $\text{Ti}_2\text{AlC}$ ,  $\text{TiB}$  and  $\text{TiB}_2$  particles dispersed in the whole volume of the ingots.
2. The shape of  $\text{Ti}_2\text{AlC}$  particles in the central part of the ingots is elongated. The volume fraction of the carbide particles increases with the amount of carbon from 8 to 18 vol.%. In the vicinity of the surface of ingots, long thin needle shaped carbide particles are formed mainly in the ingots with lower amounts of carbon (3-5 at.%). Large clusters of small rod shaped carbide particles are observed in the alloys with 5 and 7 at.% of C.
3. The lamellar grains in the central part of the ingots maintain the elongated shape of the carbide particles. The orientation of  $\alpha_2+\gamma$  lamellae is parallel to the longitudinal axis of the carbide particles in the majority of grains.
4. Carbon is distributed inhomogenously in the carbide particles and in the matrix. The core of the large  $\text{Ti}_2\text{AlC}$  particles is enriched by carbon and depleted by Al in all studied ingots. The increase of C content in the vicinity of  $\gamma/\beta$  interface and along grain boundaries is detected.
5. The average Vickers hardness of the studied alloys and Vickers microhardness of lamellar grains,  $\beta$ -phase and carbide particles don't show the significant variations with the carbon content. The hardness considerably exceeds the average values in the surface regions with small rod shape particles densely distributed in the matrix with nearly equiaxed grains.

### Acknowledgements

This work is the result of the projects of the Slovak Research and Development Agency under the contract APVV-15-0660 and APVV-0434-10. The financial support of the Slovak Grant Agency for Science under the contract VEGA 2/0125/16 is acknowledged.

### References

- [1] Kothari K, Radhakrishnan R and Wereley N M 2012 *Prog. Aerosp. Sci.* **55** 1
- [2] Clemens H and Mayer S 2013 *Adv. Eng. Mater.* **15** 191
- [3] Appel F, Paul J D H and Oehring M 2011 *Gamma Titanium Aluminide Alloys* (Wiley-VCH Verlag & Co. KGaA) 277
- [4] Kevorkijan V and Škapin S D 2009 *Metall. Mater. Eng.* **15** 75
- [5] Schwaighofer E, Rashkova B, Clemens H, Stark A and Mayer S 2014 *Intermetallics* **46** 173
- [6] Kamyshnykova K and Lapin J 2016 *Proc. 6<sup>th</sup> Int. Conf. MTSM 2016 (Split)* 67
- [7] Song X J, Cui H Z, Hou N, Wei N, Han Y, Tian J and Song Q 2016 *Intermetallics* **42** 13586
- [8] Klein T, Schachermayer M, Mendez-Martin F, Schöberl T, Rashkova B, Clemens H and Mayer S 2015 *Acta Mater.* **94** 205
- [9] Scheu C, Stergar E, Schober M, Cha L, Clemens H, Bartels A, Schimansky F P and Cerezo A 2009 *Acta Mater.* **57** 1504
- [10] Cao L, Wang H W, Zou C M and Wei Z J 2009 *J. Alloys Compd.* **484** 816
- [11] Wei Z, Wang H, Jin Y, Zhang H and Zeng S 2002 *J. Mater. Sci.* **27** 1809